Atmos. Chem. Phys. Discuss., 15, 14141–14169, 2015
www.atmos-chem-phys-discuss.net/15/14141/2015/
doi:10.5194/acpd-15-14141-2015

Atmospheric Chemistry and Physics Discussions

Black carbon aerosol in winter northeastern Qinghai-Tibetan Plateau, China: the effects from South Asia pollution

Q. Y. Wang[1], R.-J. Huang[1,2,3], J. J. Cao[1,5], X. X. Tie[1], H. Y. Ni[1], Y. Q. Zhou[1], Y. M. Han[1], T. F. Hu[1], C. S. Zhu[1], T. Feng[4,5], N. Li[6], and J. D. Li[1]

[1]Key Laboratory of Aerosol Chemistry and Physics, Institute of Earth Environment, Chinese Academy of Sciences, Xi'an 710061, China
[2]Laboratory of Atmospheric Chemistry, Paul Scherrer Institute (PSI), 5232 Villigen, Switzerland
[3]Centre for Climate and Air Pollution Studies, Ryan Institute, National University of Ireland Galway, University Road, Galway, Ireland
[4]School of Human Settlements and Civil Engineering, Xi'an Jiaotong University, Xi'an 710054, China
[5]Institute of Global Environmental Change, Xi'an Jiaotong University, Xi'an 710049, China
[6]National Taiwan University, Department of Atmospheric Science, Taipei 10617, Taiwan

Received: 25 March 2015 – Accepted: 25 April 2015 – Published: 19 May 2015

Correspondence to: R.-J. Huang (rujin.huang@psi.ch) and J. J. Cao (cao@loess.llqg.ac.cn)

Published by Copernicus Publications on behalf of the European Geosciences Union.

Abstract

Black carbon (BC) aerosol at high-altitude Qinghai-Tibetan Plateau has potential effects on the regional climate and hydrological cycle. An intensive measurement campaign was conducted at Qinghai Lake (~ 3200 a.s.l.) at the edge of the northeastern Qinghai-Tibetan Plateau during winter using a ground-based single particle soot photometer (SP2) and a photoacoustic extinctiometer (PAX). The average BC concentration and number fraction of coated BC were found to be $160 \pm 190\,\mathrm{ng\,m^{-3}}$ and 59.3 % for the entire campaign, respectively. Significant enhancements of BC loadings and number fraction of coated BC were observed during pollution episode, with an average value of $390\,\mathrm{ng\,m^{-3}}$ and 64.6 %, respectively. The mass size distribution of BC particles showed lognormal distribution with a peak diameter of ~ 187 nm regardless of the pollution level. Five-day backward trajectory analysis combined with the fire counts map suggests that the biomass burning air masses from North India contributing to the increased BC loadings during the campaign. The potential source contribution function (PSCF) model further proves that North India is an important potential region influencing northeastern Qinghai-Tibetan Plateau during the pollution episode. The BC mass absorption cross section (MAC_{BC}) at $\lambda = 532$ nm was slightly larger during pollution episode ($10.2\,\mathrm{m^2\,g^{-1}}$) than in clean days ($8.9\,\mathrm{m^2\,g^{-1}}$), likely due to the higher mixing state of BC with other chemical components during pollution episode. The number fraction of coated BC particles showed positive correlation with light absorption, suggesting that the increase of coated BC particles will enhance the light absorption. The estimated BC direct radiative forcing was + $0.93\,\mathrm{W\,m^{-2}}$ for pollution episode, which is 2 times larger than that in clean days. Our study provides insight into the potential climatic impacts of BC aerosol transported to the Qinghai-Tibetan Plateau from South Asian regions, and is also useful for future modeling studies.

ACPD
15, 14141–14169, 2015

1 Introduction

Black carbon (BC) aerosol has received worldwide concern due to its effects on climate and human health (Anenberg et al., 2012; Bond et al., 2013). BC shows an overall warming effect by either absorbing incoming solar radiation in the atmosphere or by reducing the albedo of surface (i.e., snow and ice) (Jacobson, 2001; Ramanathan and Carmichael, 2008; Kühn et al., 2014). A total climate forcing of BC particles is estimated to be $+1.1\,\mathrm{W\,m^{-2}}$, which is ranked as the second largest contributor to anthropogenic radiative forcing after carbon dioxide in the present-day atmosphere (Bond et al., 2013). BC particles, derived from incomplete combustion of fossil fuels or biomass, are mainly hydrophobic when emitted, but become hygroscopic over time due to atmospheric aging processes. When BC particles are mixed with water-soluble aerosol composition, they can serve as cloud condensation nuclei and therefore affect microphysical properties of clouds leading to indirect effect on climate (Hansen et al., 2005; Lohmann and Feichter, 2005). Moreover, the impacts of BC aerosols on the radiative balance may lead to far-reaching consequences, such as global dimming (Wild et al., 2007), lower crop yields (Tollefsen et al., 2009), and negative impacts on terrestrial and aquatic ecosystems (Forbes et al., 2006).

The Qinghai-Tibetan Plateau is known as the "Third Pole" of the Earth because of its immense area and high elevation. It covers the area of 27–45° N, 70–105° E with an average elevation > 4000 m a.s.l. Due to the special landform, ecosystem and monsoon circulation, the Qinghai-Tibetan Plateau exerts profound effects on regional and global radiative budget and climate (Kopacz et al., 2011; Su et al., 2013; Yang et al., 2014). The Qinghai-Tibetan Plateau is surrounded by many important anthropogenic BC aerosol source areas (Zhang et al., 2009), such as South Asia (e.g., India) and East Asia (e.g., China). Inventory study suggests that the BC emissions in China and India have increased by 40 and 54 % from 2000 to 2008, respectively (Kurokawa et al., 2013). Due to the general circulation patterns, the Qinghai-Tibetan Plateau becomes a strong receptor of these high BC source areas (Cao et al., 2010; Xia et al., 2011; Cong et al.,

ACPD
15, 14141–14169, 2015

2013; Zhao et al., 2013). Lu et al. (2012) shows that South Asia and East Asia are the main source regions, accounting for 67 and 17 % of BC transported to the Himalayas and Qinghai-Tibetan Plateau on an annual basis, followed by former USSR (~ 8 %), Middle East (~ 4 %), Europe (~ 2 %), and Northern Africa (~ 1 %). Deposition of BC on snow and ice at the Qinghai-Tibetan Plateau would decrease the snow surface albedo (Xu et al., 2012; Ming et al., 2013). The Qinghai-Tibetan Plateau Glaciers, which are the largest glaciers outside of the Polar Regions, have shown signs of retreat (Xu et al., 2009). The snowmelt from Qinghai-Tibetan Plateau vitally affects the sustaining seasonal water availability leading to agriculture security in South, East, and Southeast Asia (Immerzeel et al., 2010).

The effect of BC transported from surroundings on Qinghai-Tibetan's environment and climate is of great significance. However, BC studies are still very scarce to date in the Qinghai-Tibetan Plateau (e.g., Cao et al., 2010; Zhao et al., 2013; Wang et al., 2014a). In these limited studies, online and offline filter-based techniques are often used. Due to inherent systematic limitations, direct examination of BC size distribution and mixing state with filter-based measurements is not feasible (Watson et al., 2005; Slowik et al., 2007; Collaud Coen et al., 2010; Bond et al., 2013). The BC optical properties are dependent on its physical (e.g., size and shape) and chemical (e.g., mixing with other materials) features. For example, the degree of enhancement in mass absorption cross section from internal mixture of BC with other aerosol components can lead to large difference in the prediction of global radiative budget (Bond et al., 2006; Chung et al., 2012; Zhuang et al., 2013). Consequently, accurate characterization of BC particles is crucial for a precise estimate of the impacts of BC on the atmospheric radiative forcing, human health, and air quality. In this study, a single particle soot photometer (SP2) and a photoacoustic extinctiometer (PAX) were used to investigate the BC mass concentrations, size distribution, mixing state, and aerosol light absorption properties in northeastern Qinghai-Tibetan Plateau. The primary objectives of this study were (1) to investigate the important potential BC source regions responsible for the high wintertime BC concentration in the Northeastern Qinghai-Tibetan Plateau, (2)

ACPD
15, 14141–14169, 2015

to study the effect of BC mixing state on light absorption properties, (3) to estimate the direct radiative forcing during BC pollution episode.

2 Methodology

2.1 Measurement site

Qinghai Lake (36.53–37.25° N and 99.6–100.78° E), the largest saline lake in China, is located ~ 3200 m a.s.l. in a drainage closed intermountain basin on the Northeast Qinghai-Tibetan Plateau with an area of ~ 4400 km^2 (Fig. 1). This region is highly sensitive to global climate change, because it is situated in the sensitive semi-arid zone between the Asian monsoon-controlled area and the westerly jet stream-influenced area (An et al., 2012). Intensive measurements were taken from 16–27 November 2012 from the rooftop (~ 15 m a.g.l.) of a sampling tower at the "Bird Island" peninsula (36.98° N, 99.88° E), which is located at the northwest section of the Qinghai Lake shore as shown in Fig. 1.

2.2 BC mass and mixing state measurements

The commercially available SP2 instrument (Droplet Measurement Technology, Boulder, CO, USA) has proven useful for measuring BC mass, size, and mixing state (e.g., Gao et al., 2007; Moteki and Kondo, 2007; Schwarz et al., 2010; Wang et al., 2014b). The operating principles of the SP2 are described elsewhere (Stephens et al., 2003; Schwarz et al., 2006). Briefly, the SP2 relies on laser-induced incandescence to quantify the BC mass of individual particles. Continuous intracavity Nd:YAG laser light at 1064 nm is used to heat BC-containing particles to their vaporization point. The peak incandescence signal is linearly related to the BC mass in the particle irrespective of the particle morphology or mixing state; this holds true over most of the BC mass range typically observed in the accumulation mode (Slowik et al., 2007). In this work,

ACPD
15, 14141–14169, 2015

the BC mass in the range of ~ 0.4–1000 fg, equivalent to ~ 70–1000 nm volume equivalent diameter, is quantified, assuming a void-free density of 2.0 g cm^{-3} (Schwarz et al., 2008a). This range covers > 90 % of the BC mass in the accumulation mode. Note that the SP2 only quantifies the most refractory and most efficient light-absorbing component of combustion aerosol. The BC concentration is adjusted to standard temperature and pressure (STP, $T_{standard}$ = 273.15 K and $P_{standard}$ = 1013.25 hPa). More details about the SP2 calibration and uncertainty can be found in our previous work (Wang et al., 2014a).

The SP2 is capable of determining the BC mixing state. The time delay between the peaks from the scattered light and incandescence signals is an indicator of the amount of non-BC material mixed internally with individual BC particles (Schwarz et al., 2006; McMeeking et al., 2011; Perring et al., 2011; Wang et al., 2014a). This method is sensitive to optically significant amounts of non-BC material. The time delay occurs because the coatings must be removed from the BC particle before the onset of incandescence. The number fraction of coated BC particles which is calculated from the distribution of time delay is an indicator of the degree to which the BC particles are coated with other substances. This number fraction is higher for more aged BC particles due to the formation of coating from atmospheric processes.

2.3 Particle light absorption measurements

The PAX (Droplet Measurement Technology, Boulder, CO, USA) measures light absorption and scattering coefficients simultaneously using a modulated diode laser. The light absorption coefficient is measured based on the intracavity photoacoustic technology. A laser beam in the acoustic chamber of the instrument heats suspended absorbing particles, by which a pressure wave is produced and detected with a sensitive microphone. A wide-angle integrating reciprocal nephelometer in the acoustic chamber measures the light scattering coefficient regardless of the particles' chemical makeup, mixing state, or morphology. In this study, the light absorption at λ = 532 nm is measured. Before sampling, nitrogen dioxide and ammonium sulfate are used for

ACPD
15, 14141–14169, 2015

the calibration of light absorption and scattering. Like SP2 measurement, the absorption measurement reported here is also corrected for the standard temperature and pressure.

3 Results and discussion

3.1 Mass, size and mixing state of BC aerosol

The time series of hourly averaged BC mass concentrations and the mixing state obtained during the campaign are shown in Fig. 2, and a statistical summary of the data is presented in Table 1. The mean concentration of BC aerosol (± SD) was $160 \pm 190\,\mathrm{ng\,m^{-3}}$ during the entire campaign period, ranging from 6 to $1040\,\mathrm{ng\,m^{-3}}$. The mean number fraction of coated BC is found to be 59.3 ± 6.9 % (range 39.8–73.2 %), suggesting the majority of aged and thickly-coated BC particles in wintertime in the Qinghai Lake region. It is found that ~ 30 % of the BC values are higher than the mean value, and the variation coefficient (defined by SD/mean) of BC values reaches as high as 120 %, suggesting a large BC burden even at the free tropospheric altitude. Elevated BC concentration was observed from 19 to 21 November (defined as a pollution episode hereafter) with an average BC loading of $390\,\mathrm{ng\,m^{-3}}$, which is about 4 times higher than that from the rest of measurement period ($86\,\mathrm{ng\,m^{-3}}$, defined as clean days). The mean number fraction of coated BC also increases to 64.6 % during the pollution episode, higher than that in the clean days (57.7 %). Given that local BC emissions in the Qinghai Lake region and even the entire Qinghai-Tibetan Plateau are very limited, the enhanced BC concentrations observed during this campaign are most likely from regional transport as discussed below.

Figure 3 shows the mass size distribution of BC particles for the entire campaign period. A lognormal size distribution pattern in volume equivalent diameter (VED, for the size of BC core of a particle) is found, with a very close peak diameter for BC pollution episode (188 nm) and clean days (187 nm). The size distributions of BC core in the

ACPD
15, 14141–14169, 2015

ambient atmosphere are affected by the size of fresh BC particles and the subsequent atmospheric processing (Bond et al., 2013). The growth of BC particles is a complex process, including water accretion, coagulation, condensation, and the accumulation of other materials through heterogeneous reactions. However, only the process of coagulation can lead to the increase of BC core in VED. The coagulation of particles in ambient air is dominated by Brownian motion, a slow process for particles in the accumulation mode (Seinfeld and Pandis, 1998). Therefore, it is reasonable to understand the similarity in VED size distribution for BC core between clean and pollution episode.

3.2 BC potential pollution source areas

To examine the contribution of regional transport, the hybrid single-particle Lagrangian integrated trajectories (HYSPLIT) model (www.arl.noaa.gov/reday.html) was used to compute the five-day back trajectories using BC as a marker. The five-day period is chosen because the atmospheric lifetime of BC is typically in the order of one week (Chung and Seinfeld, 2005; Cape et al., 2012). Figure 4a shows the results of backward trajectories calculated at 00:00, 06:00, 12:00, and 18:00 local stand time (LST) with the arrival height of 500 m a.g.l. During BC pollution episode, the air masses were mainly originated from the regions of high BC emissions in North India (Sahu et al., 2008), which then passed over the rather clean western Qinghai-Tibetan Plateau (Zhang et al., 2009). In contrast, the air masses were originated from Europe and passed through the western part of China during clean days. An aerosol optical depth (AOD) map, retrieved from the measurements of Moderate Resolution Imaging Spectroradiometer (MODIS) on the Terra satellite, describes the mean atmospheric aerosol loading around Qinghai-Tibetan Plateau (Fig. 5a). Since 5 day back trajectory analysis shows that the polluting air masses arriving the measurement site on 19–21 November were from North India, the pollution status of North India on 14–16 November (i.e., 5 days backward) was examined. As shown in Fig. 5a, high AOD values can be found along the Indo-Gangetic Basin in India and South Pakistan, indicating heavy pollution in this region. The fire counts map obtained from MODIS observation on NASA satellites also shows a large

ACPD
15, 14141–14169, 2015

number of biomass burning activities in North India during 14–16 November, indicating large biomass burning aerosol (including BC aerosol) emissions. Although the high altitude of the Himalayas was thought to be a physical wall for atmospheric pollutants, previous studies indicate that the high Himalayan valleys can act as a "direct channel" for the transport of air pollutants up to 5000 m a.s.l. (e.g., Bonasoni et al., 2010). After reaching the north of the Himalayan, the air pollutants can further transport to the central Qinghai-Tibetan Plateau (Hindman and Upadhyay, 2002; Xia et al., 2011). Therefore, the BC pollution episode observed in the Qinghai Lake measurement site is most likely derived from the biomass burning emissions in North India.

The potential source contribution function (PSCF) model (e.g., Wang et al., 2006) was used to further explore the potential source regions which influence BC concentration in the Qinghai Lake region. To do so, the geographic region covered by the trajectories was divided into an array of $0.5^\circ \times 0.5^\circ$ grid cells. The PSCF values for the grid cells were calculated by counting the trajectory segment endpoints that terminate within each cell. The number of endpoints that fall in the ijth cell is designated as n_{ij}. The number of endpoints for the same cell corresponding to BC concentrations higher than an arbitrarily set criterion is defined to be m_{ij}. Then, the PSCF value for the ijth cell is defined as: $\mathrm{PSCF}_{ij} = m_{ij}/n_{ij}$. Because of the impact of small values of n_{ij}, an arbitrary weight function W_{ij} was used to better reflect the uncertainty in the values for these cells (Polissar et al., 1999). The weight function reduces the PSCF values when the total number of the endpoints in a particular cell is less than about three times the average value of the end points per each cell. Here, W_{ij} is defined as (Polissar et al., 2001):

$$W_{ij} = \begin{cases} 1.00 & 80 < n_{ij} \\ 0.70 & 20 < n_{ij} \le 80 \\ 0.42 & 10 < n_{ij} \le 20 \\ 0.05 & n_{ij} \le 10 \end{cases} \quad (1)$$

ACPD
15, 14141–14169, 2015

Although PSCF model is often used to determine the potential source regions (e.g., Wang et al., 2006; Heo et al., 2013; Zhang et al., 2013), a limitation of this model is that grid cells can have the same PSCF value when sample concentrations at the receptor site are either only slightly higher or extremely higher than the criterion. This may lead to difficulties in distinguishing moderate sources from strong ones. To compensate for this limitation, the PSCF result calculated from the 75th percentile of all the data is set as the criterion ($170\,ng\,m^{-3}$) in this study. Figure 4b shows the map of PSCF results for the entire campaign period. High PSCF values are found at North India, likely due to the biomass burning emissions as discussed above. The PSCF values are low in the Qinghai Lake and surrounding regions, indicating lower likelihood of BC emissions from local sources compared to regional transport from North India.

3.3 Optical properties of BC aerosol

The hourly light absorption coefficient varied from 0.0 to $18.1\,M\,m^{-1}$ with an average value of $2.1 \pm 2.4\,M\,m^{-1}$ for the entire campaign (Table 1). The average value increased to $3.7 \pm 2.9\,M\,m^{-1}$ during BC pollution episode, which is ~ 3 times higher than the average value in clean days ($1.3 \pm 1.6\,M\,m^{-1}$). The BC mass absorption cross section (MAC_{BC}, expressed here in $m^2\,g^{-1}$) is one of the most important optical properties for BC aerosol because this parameter links optical properties to BC mass. Linear correlations between absorption coefficients at $\lambda = 532\,nm$ derived from the PAX measurement and BC mass loadings from the SP2 measurement during BC pollution episode and clean days are shown in Fig. 6. The high correlation coefficients (0.92 for pollution episode and 0.82 for clean days) indicate consistent response of the measurements. The slopes, which represent MAC_{BC} at $\lambda = 532\,nm$, are $10.2\,m^2\,g^{-1}$ for BC pollution episode and $8.9\,m^2\,g^{-1}$ for clean days. The enhanced MAC_{BC} during BC pollution episode could be attributed to the higher mixing state of BC with other particulate non-light-absorbing components, which have the potential to enhance the absorption property of BC particles (Bond et al., 2006). It is interesting to note that the intercept of the fitting line in Fig. 6 is close to zero for BC pollution episode, but relative large

ACPD
15, 14141–14169, 2015

for clean days. Previous studies demonstrate that black carbon, brown carbon and mineral dust are the three most important light-absorbing aerosol composition in the atmosphere (Yang et al., 2009) and that they can absorb light at visible wavelength (e.g., λ = 532 nm) although their light absorption properties are distinctive functions of the light wavelengths (Lack and Cappa, 2010; Yang et al., 2009). The small intercept during BC pollution episode therefore suggests that BC particles are the main contributor to light absorption, while the large intercept during clean days suggests the existence of other light absorption materials (e.g., brown carbon) besides BC particles during the measurement period.

Both laboratory studies and field measurements have shown that the BC light absorption (related to its direct radiative effects) can be enhanced by a factor of 1.5–2.0 when BC particles are internally mixed with other non-light-absorbing aerosol components including sulfate, nitrate, organics and water (e.g., Bond et al., 2006; Shiraiwa et al., 2010; Wang et al., 2014b). This is because the non-absorbing materials act like a lens and therefore refract the light toward the absorbing BC core, leading to the enhancement of absorption on visible light. Figure 7 shows the relationship among light absorption, BC mass and mixing state for the entire campaign. It can be seen from the figure that the light absorption coefficients generally increase with increasing number fraction of coated BC with the latter being positively correlated with the BC mass concentration. Such correlation indicates that the outflow from polluted south Asia would increase the BC mass concentration leading to light absorption enhancement on the one hand, and the increased number fraction of coated BC particles would further enhance the light absorption on the other hand. Compared to the MAC_{BC} of 7.8 $m^2\,g^{-1}$ (interpolated to 532 from 550 nm assuming an Absorption Ångström Exponent of 1.0) suggested by Bond and Bergstrom (2006) for uncoated BC particles, the MAC_{BC} increased ~ 30 % during BC pollution episode. This is consistent with previous studies that a complete encapsulation of a BC core with non-light-absorbing materials could lead to an absorption enhancement of up to 30–50 % (Fuller et al., 1999; Bond et al., 2006; Schwarz et al., 2008b).

ACPD
15, 14141–14169, 2015

3.4 Implications for direct radiative forcing

The direct radiative forcing of BC particles (DRF_{BC}) refers to the change in energy balance at the top of the atmosphere due to absorption and scattering of sunlight by BC particles. Here the DRF_{BC} is estimated from a simple analytical solution derived from the following parameterization (Chylek and Wong, 1995):

$$DRF_{BC} = \frac{S_0}{4} T_{atm}^2 \times (1 - N) \times \left[4\alpha\delta_{ab} - 2 \times (1 - \alpha)^2 \beta\delta_{sc}\right] \quad (2)$$

where S_0 is the solar irradiance (1370 $W m^{-2}$), T_{atm} is the atmospheric transmission (0.79), N is the cloud fraction (0.6), a is the surface albedo (i.e., 0.18 at rural region), β is the backscatter fraction, which is assumed to be 0.17 (Kim et al., 2012), and δ_{ab} and δ_{sc} are the absorption and scattering optical depth, respectively. The daily values of δ_{ab} and δ_{sc} are estimated from Aura-OMI satellite measurements (http://disc.sci.gsfc.nasa.gov/). More details about the assumption of this equation can be found in Kim et al. (2012). The average DRF_{BC} is estimated to be 0.6 ± 0.4 $W m^{-2}$ for the entire campaign, ranging from 0.05 to 1.6 $W m^{-2}$. During BC pollution episode, the DRF_{BC} was 0.93 ± 0.57 $W m^{-2}$, which is about two times higher than that in clean days (0.48 ± 0.29 $W m^{-2}$). It should be noted that the DRF_{BC} is calculated based on the assumption that BC particles are externally mixed with other non-light-absorbing particles. Given that a fraction of BC particles may be internally mixed with other aerosol compounds, the DRF_{BC} calculated here should be considered as the lower limit. Therefore, the BC mediated radiative forcing is of great importance for the local atmospheric radiative balance in the northeastern Qinghai-Tibetan Plateau. Given the much shorter lifetime of BC aerosol compared with greenhouse gases, mitigation of BC pollution could be an efficient control strategy for protecting the vulnerable environment in the Qinghai-Tibetan Plateau because it reduces the radiative forcing directly by reducing the BC particle concentration and indirectly by slowing down the melting of snowpack and ice that can reflect the sunlight.

ACPD
15, 14141–14169, 2015

4 Conclusions

The mass concentration, size distribution, mixing state and optical properties of BC particles in the Qinghai Lake region of the Qinghai-Tibetan Plateau are studied. The results show that average BC concentration and number fraction of coated BC are $160 \pm 190\,\mathrm{ng\,m^{-3}}$ and 59.3 %, respectively, for the entire campaign in November 2012. The average BC mass concentration is about 4 times larger for pollution episode than for clean days; and the number fraction of coated BC particles also increases from 57.7 % for clean days to 64.6 % for pollution episode. The mass size distribution of BC particles shows lognormal distribution with a peak diameter of ~ 187 nm regardless of the pollution level. Back trajectory analysis and potential source contribution function (PSCF) model study show that North India is an important region influencing the BC level in the northeastern Qinghai-Tibetan Plateau during the pollution episode. The fire counts map also suggests that the pollution episode is likely caused by biomass burning in North India.

The light absorption coefficient (at $\lambda = 532$ nm) shows strong positive correlation with the BC loading. The average value is $1.3\,\mathrm{M\,m^{-1}}$ for the clean days and increases to $3.7\,\mathrm{M\,m^{-1}}$ for pollution episode. The BC mass absorption cross section ($\mathrm{MAC_{BC}}$) is $10.2\,\mathrm{m^2\,g^{-1}}$ for BC pollution episode, which is about 30 % larger than uncoated BC particles. The number fraction of coated BC particles shows positive correlation with light absorption, suggesting the increase of aged BC particles increases the light absorption. The estimated BC direct radiative forcing is about 2 times higher for pollution episode ($0.93 \pm 0.57\,\mathrm{W\,m^{-2}}$) than for clean days ($0.48 \pm 0.29\,\mathrm{W\,m^{-2}}$).

This case study provides an insight into the South Asia pollution impacting northeast Qinghai-Tibetan Plateau through long-range transport. The increased BC loadings not only disturb the energy budget of the atmosphere in this region, but also modify the snow albedo by deposition. This in turn can accelerate the melting of the glaciers and snow-pack over Qinghai-Tibetan and, thus, affect the sustaining seasonal water availability leading to security of agriculture in downstream regions. More studies need to be

ACPD
15, 14141–14169, 2015

addressed on the basis of long-period investigations in the Qinghai-Tibetan Plateau regions to improve our scientific understanding of the regional climate on the inter-annual as well as intra-seasonal scale.

Acknowledgements. This work was supported by the projects from the National Natural Science Foundation of China (41230641) and the Ministry of Science and Technology (2012BAH31B03, 201209007).

References

An, Z., Colman, S. M., Zhou, W., Li, X., Brown, E. T., Jull, A. J. T., Cai, Y., Huang, Y., Lu, X., Chang, H., Song, Y., Sun, Y., Xu, H., Liu, W., Jin, Z., Liu, X., Cheng, P., Liu, Y., Ai, L., Li, X., Liu, X., Yan, L., Shi, Z., Wang, X., Wu, F., Qiang, X., Dong, J., Lu, F., and Xu, X.: Interplay between the Westerlies and Asian monsoon recorded in Lake Qinghai sediments since 32 ka, Sci. Rep., 2, 619, doi:10.1038/srep00619, 2012.

Anenberg, S. C., Schwartz, J., Shindell, D., Amann, M., Faluvegi, G., Klimont, Z., Janssens-Maenhout, G., Pozzoli, L., Van Dingenen, R., Vignati, E., Emberson, L., Muller, N. Z., West, J. J., Williams, M., Demkine, V., Hicks, W. K., Kuylenstierna, J., Raes, F., and Ramanathan, V.: Global air quality and health co-benefits of mitigating near-term climate change through methane and black carbon emission controls, Environ. Health Persp., 120, 831–839, 2012.

Bonasoni, P., Laj, P., Marinoni, A., Sprenger, M., Angelini, F., Arduini, J., Bonafè, U., Calzolari, F., Colombo, T., Decesari, S., Di Biagio, C., di Sarra, A. G., Evangelisti, F., Duchi, R., Facchini, MC., Fuzzi, S., Gobbi, G. P., Maione, M., Panday, A., Roccato, F., Sellegri, K., Venzac, H., Verza, GP., Villani, P., Vuillermoz, E., and Cristofanelli, P.: Atmospheric Brown Clouds in the Himalayas: first two years of continuous observations at the Nepal Climate Observatory-Pyramid (5079 m), Atmos. Chem. Phys., 10, 7515–7531, doi:10.5194/acp-10-7515-2010, 2010.

Bond, T. C. and Bergstrom, R. W.: Light absorption by carbonaceous particles: an investigative review, Aerosol Sci. Tech., 40, 27–67, 2006.

Bond, T. C., Doherty, S. J., Fahey, D. W., Forster, P. M., Berntsen, T., DeAngelo, B. J., Flanner, M. G., Ghan, S., Kärcher, B., Koch, D., Kinne, S., Kondo, Y., Quinn, P. K., Sarofim, M. C.,

ACPD
15, 14141–14169, 2015

Schultz, M. G., Schulz, M., Venkataraman, C., Zhang, H., Zhang, S., Bellouin, N., Guttikunda, S. K., Hopke, P. K., Jacobson, M. Z., Kaiser, J. W., Klimont, Z., Lohmann, U., Schwarz, J. P., Shindell, D., Storelvmo, T., Warren, S. G., and Zender, C. S.: Bounding the role of black carbon in the climate system: a scientific assessment, J. Geophys. Res., 118, 5380–5552, 2013.

Bond, T. C., Habib, G., and Bergstrom, R. W.: Limitations in the enhancement of visible light absorption due to mixing state, J. Geophys. Res., 111, D20211, doi:10.1029/2006JD007315, 2006.

Cao, J. J., Tie, X. X., Xu, B. Q., Zhao, Z. Z., Zhu, C. S., Li, G. H., and Liu, S. X.: Measuring and modeling black carbon (BC) contamination in the SE Tibetan Plateau, J. Atmos. Chem., 67, 45–60, 2010.

Cape, J. N., Coyle, M., and Dumitrean, P.: The atmospheric lifetime of black carbon, Atmos. Environ., 59, 256–263, 2012.

Chung, C. E., Lee, K., and Mueller, D.: Effect of internal mixture on black carbon radiative forcing, Tellus B, 64, 1–13, 2012.

Chung, S. H. and Seinfeld, J. H.: Climate response of direct radiative forcing of anthropogenic black carbon, J. Geophys. Res., 110, D11102, doi:10.1029/2004JD005441, 2005.

Chylek, P. and Wong, J.: Effect of absorbing aerosols on global radiation budget, Geophys. Res. Lett., 22, 929–931, 1995.

Collaud Coen, M., Weingartner, E., Apituley, A., Ceburnis, D., Fierz-Schmidhauser, R., Flentje, H., Henzing, J. S., Jennings, S. G., Moerman, M., Petzold, A., Schmid, O., and Baltensperger, U.: Minimizing light absorption measurement artifacts of the Aethalometer: evaluation of five correction algorithms, Atmos. Meas. Tech., 3, 457–474, doi:10.5194/amt-3-457-2010, 2010.

Cong, Z., Kang, S., Gao, S., Zhang, Y., Li, Q., and Kawamura, K.: Historical trends of atmospheric black carbon on Tibetan Plateau as reconstructed from a 150 Year lake sediment record, Environ. Sci. Technol., 47, 2579–2586, 2013.

Forbes, M. S., Raison, R. J., and Skjemstad, J. O.: Formation, transformation and transport of black carbon (charcoal) in terrestrial and aquatic ecosystems, Sci. Total Environ., 370, 190–206, 2006.

Fuller, K. A., Malm, W. C., and Kreidenweis, S. M.: Effects of mixing on extinction by carbonaceous particles, J. Geophys. Res., 104, 15941–15954, 1999.

ACPD
15, 14141–14169, 2015

Gao, R., Schwarz, J., Kelly, K., Fahey, D., Watts, L., Thompson, T., Spackman, J., Slowik, J., Cross, E., and Han, J. H.: A novel method for estimating light-scattering properties of soot aerosols using a modified single-particle soot photometer, Aerosol Sci. Tech., 41, 125–135, 2007.

Hansen, J., Sato, M., Ruedy, R., Nazarenko, L., Lacis, A., Schmidt, G. A., Russell, G., Aleinov, I., Bauer, M., Bauer, S., Bell, N., Cairns, B., Canuto, V., Chandler, M., Cheng, Y., Del Genio, A., Faluvegi, G., Fleming, E., Friend, A., Hall, T., Jackman, C., Kelley, M., Kiang, N., Koch, D., Lean, J., Lerner, J., Lo, K., Menon, S., Miller, R., Minnis, P., Novakov, T., Oinas, V., Perlwitz, J., Rind, D., Romanou, A., Shindell, D., Stone, P., Sun, S., Tausnev, N., Thresher, D., Wielicki, B., Wong, T., Yao, M., and Zhang, S.: Efficacy of climate forcings, J. Geophys. Res., 110, D18104, doi:10.1029/2005JD005776, 2005.

Heo, J., McGinnis, J. E., de Foy, B., and Schauer, J. J.: Identification of potential source areas for elevated $PM_{2.5}$, nitrate and sulfate concentrations, Atmos. Environ., 71, 187–197, 2013.

Hindman, E. E. and Upadhyay, B. P.: Air pollution transport in the Himalayas of Nepal and Tibet during the 1995–1996 dry season, Atmos. Environ., 36, 727–739, 2002.

Immerzeel, W. W., van Beek, L. P. H., and Bierkens, M. F. P.: Climate change will affect the Asian water towers, Science, 328, 1382–1385, 2010.

Jacobson, M. Z.: Strong radiative heating due to the mixing state of black carbon in atmospheric aerosols, Nature, 409, 695–697, 2001.

Kühn, T., Partanen, A. I., Laakso, A., Lu, Z., Bergman, T., Mikkonen, S., Kokkola, H., Korhonen, H., Räisänen, P., Streets, D. G., Romakkaniemi, S., and Laaksonen, A.: Climate impacts of changing aerosol emissions since 1996, Geophys. Res. Lett., 41, 4711–4718, 2014.

Kim, M. Y., Lee, S.-B., Bae, G.-N., Park, S. S., Han, K. M., Park, R. S., Song, C. H., and Park, S. H.: Distribution and direct radiative forcing of black carbon aerosols over Korean Peninsula, Atmos. Environ., 58, 45–55, 2012.

Kopacz, M., Mauzerall, D. L., Wang, J., Leibensperger, E. M., Henze, D. K., and Singh, K.: Origin and radiative forcing of black carbon transported to the Himalayas and Tibetan Plateau, Atmos. Chem. Phys., 11, 2837–2852, doi:10.5194/acp-11-2837-2011, 2011.

Kurokawa, J., Ohara, T., Morikawa, T., Hanayama, S., Janssens-Maenhout, G., Fukui, T., Kawashima, K., and Akimoto, H.: Emissions of air pollutants and greenhouse gases over Asian regions during 2000–2008: Regional Emission inventory in ASia (REAS) version 2, Atmos. Chem. Phys., 13, 11019–11058, doi:10.5194/acp-13-11019-2013, 2013.

ACPD
15, 14141–14169, 2015

Lack, D. A. and Cappa, C. D.: Impact of brown and clear carbon on light absorption enhancement, single scatter albedo and absorption wavelength dependence of black carbon, Atmos. Chem. Phys., 10, 4207–4220, doi:10.5194/acp-10-4207-2010, 2010.
Lohmann, U. and Feichter, J.: Global indirect aerosol effects: a review, Atmos. Chem. Phys., 5, 715–737, doi:10.5194/acp-5-715-2005, 2005.
Lu, Z., Streets, D. G., Zhang, Q., and Wang, S.: A novel back-trajectory analysis of the origin of black carbon transported to the Himalayas and Tibetan Plateau during 1996–2010, Geophys. Res. Lett., 39, L01809, doi:10.1029/2011GL049903, 2012.
McMeeking, G. R., Morgan, W. T., Flynn, M., Highwood, E. J., Turnbull, K., Haywood, J., and Coe, H.: Black carbon aerosol mixing state, organic aerosols and aerosol optical properties over the United Kingdom, Atmos. Chem. Phys., 11, 9037–9052, doi:10.5194/acp-11-9037-2011, 2011.
Ming, J., Wang, P., Zhao, S., and Chen, P.: Disturbance of light-absorbing aerosols on the albedo in a winter snowpack of Central Tibet, J. Environ. Sci., 25, 1601–1607, 2013.
Moteki, N. and Kondo, Y.: Effects of mixing state on black carbon measurements by laser-induced incandescence, Aerosol Sci. Tech., 41, 398–417, 2007.
Perring, A., Schwarz, J., Spackman, J., Bahreini, R., de Gouw, J., Gao, R., Holloway, J., Lack, D., Langridge, J., and Peischl, J.: Characteristics of black carbon aerosol from a surface oil burn during the deepwater horizon oil spill, Geophys. Res. Lett., 38, L17809, doi:10.1029/2011GL048356, 2011.
Polissar, A. V., Hopke, P. K., Paatero, P., Kaufmann, Y. J., Hall, D. K., Bodhaine, B. A., Dutton, E. G., and Harris, J. M.: The aerosol at Barrow, Alaska: long-term trends and source locations, Atmos. Environ., 33, 2441–2458, 1999.
Polissar, A. V., Hopke, P. K., and Harris, J. M.: Source regions for atmospheric aerosol measured at Barrow, Alaska, Environ. Sci. Technol., 35, 4214–4226, 2001.
Ramanathan, V. and Carmichael, G.: Global and regional climate changes due to black carbon, Nat. Geosci., 1, 221–227, 2008.
Sahu, S. K., Beig, G., and Sharma, C.: Decadal growth of black carbon emissions in India, Geophys. Res. Lett., 35, L02807, doi:10.1029/2007GL032333, 2008.
Schwarz, J. P., Gao, R. S., Fahey, D. W., Thomson, D. S., Watts, L. A., Wilson, J. C., Reeves, J. M., Darbeheshti, M., Baumgardner, D. G., Kok, G. L., Chung, S. H., Schulz, M., Hendricks, J., Lauer, A., Kärcher, B., Slowik, J. G., Rosenlof, K. H., Thompson, T. L., Langford, A. O., Loewenstein, M., and Aikin, K. C.: Single-particle measurements of midlati-

ACPD
15, 14141–14169, 2015

tude black carbon and light-scattering aerosols from the boundary layer to the lower stratosphere, J. Geophys. Res., 111, D16207, doi:10.1029/2006JD007076, 2006.
Schwarz, J. P., Gao, R. S., Spackman, J. R., Watts, L. A., Thomson, D. S., Fahey, D. W., Ryerson, T. B., Peischl, J., Holloway, J. S., Trainer, M., Frost, G. J., Baynard, T., Lack, D. A., de Gouw, J. A., Warneke, C., and Del Negro, L. A.: Measurement of the mixing state, mass, and optical size of individual black carbon particles in urban and biomass burning emissions, Geophys. Res. Lett., 35, L13810, doi:10.1029/2008GL033968, 2008a.
Schwarz, J. P., Spackman, J. R., Fahey, D. W., Gao, R. S., Lohmann, U., Stier, P., Watts, L. A., Thomson, D. S., Lack, D. A., Pfister, L., Mahoney, M. J., Baumgardner, D., Wilson, J. C., and Reeves, J. M.: Coatings and their enhancement of black carbon light absorption in the tropical atmosphere, J. Geophys. Res., 113, D03203, doi:10.1029/2007JD009042, 2008b.
Schwarz, J. P., Spackman, J. R., Gao, R. S., Watts, L. A., Stier, P., Schulz, M., Davis, S. M., Wofsy, S. C., and Fahey, D. W.: Global-scale black carbon profiles observed in the remote atmosphere and compared to models, Geophys. Res. Lett., 37, L18812, doi:10.1029/2010GL044372, 2010.
Seinfeld, J. H. and Pandis, S. N.: Atmospheric Chemistry and Physics: From Air Pollution to Climate Change, Wiley, New York, 1998.
Shiraiwa, M., Kondo, Y., Iwamoto, T., and Kita, K.: Amplification of light absorption of black carbon by organic coating, Aerosol Sci. Tech., 44, 46–54, 2010.
Slowik, J. G., Cross, E. S., Han, J. H., Davidovits, P., Onasch, T. B., Jayne, J. T., Williams, L. R., Canagaratna, M. R., Worsnop, D. R., and Chakrabarty, R. K.: An inter-comparison of instruments measuring black carbon content of soot particles, Aerosol Sci. Tech., 41, 295–314, 2007.
Stephens, M., Turner, N., and Sandberg, J.: Particle identification by laser-induced incandescence in a solid-state laser cavity, Appl. Optics, 42, 3726–3736, 2003.
Su, F., Duan, X., Chen, D., Hao, Z., and Cuo, L.: Evaluation of the global climate models in the CMIP5 over the Tibetan Plateau, J. Climate, 26, 3187–3208, 2013.
Tollefsen, P., Rypdal, K., Torvanger, A., and Rive, N.: Air pollution policies in Europe: efficiency gains from integrating climate effects with damage costs to health and crops, Environ. Sci. Policy, 12, 870–881, 2009.
Wang, Q. Y., Schwarz, J. P., Cao, J. J., Gao, R. S., Fahey, D. W., Hu, T. F., Huang, R.-J., Han, Y. M., and Shen, Z. X.: Black carbon aerosol characterization in a remote area of Qinghai–Tibetan Plateau, western China, Sci. Total Environ., 479, 151–158, 2014a.

ACPD
15, 14141–14169, 2015

Wang, Q. Y., Huang, R.-J., Cao, J. J., Han, Y. M., Wang, G. H., Li, G. H., Wang, Y. C., Dai, W. T., Zhang, R. J., and Zhou, Y. Q.: Mixing state of black carbon aerosol in a heavily polluted urban area of China: implications for light absorption enhancement, Aerosol Sci. Tech., 48, 689–697, 2014b.

Wang, Y. Q., Zhang, X. Y., and Arimoto, R.: The contribution from distant dust sources to the atmospheric particulate matter loadings at XiAn, China during spring, Sci. Total Environ., 368, 875–883, 2006.

Watson, J. G., Chow, J. C., and Chen, L. W. A.: Summary of organic and elemental carbon/black carbon analysis methods and intercomparisons, Aerosol Air Qual. Res., 5, 65–102, 2005.

Wild, M., Ohmura, A., and Makowski, K.: Impact of global dimming and brightening on global warming, Geophys. Res. Lett., 34, L04702, doi:10.1029/2006GL028031, 2007.

Xia, X., Zong, X., Cong, Z., Chen, H., Kang, S., and Wang, P.: Baseline continental aerosol over the central Tibetan plateau and a case study of aerosol transport from South Asia, Atmos. Environ., 45, 7370–7378, 2011.

Xu, B., Cao, J., Hansen, J., Yao, T., Joswia, D. R., Wang, N., Wu, G., Wang, M., Zhao, H., and Yang, W.: Black soot and the survival of Tibetan glaciers, P. Natl. Acad. Sci. USA, 106, 22114–22118, 2009.

Xu, B., Cao, J., Joswiak, D. R., Liu, X., Zhao, H., and He, J.: Post-depositional enrichment of black soot in snow-pack and accelerated melting of Tibetan glaciers, Environ. Res. Lett., 7, 014022, doi:10.1088/1748-9326/7/1/014022, 2012.

Yang, K., Wu, H., Qin, J., Lin, C., Tang, W., and Chen, Y.: Recent climate changes over the Tibetan Plateau and their impacts on energy and water cycle: a review, Global Planet. Change, 112, 79–91, 2014.

Yang, M., Howell, S. G., Zhuang, J., and Huebert, B. J.: Attribution of aerosol light absorption to black carbon, brown carbon, and dust in China – interpretations of atmospheric measurements during EAST-AIRE, Atmos. Chem. Phys., 9, 2035–2050, doi:10.5194/acp-9-2035-2009, 2009.

Zhang, Q., Streets, D. G., Carmichael, G. R., He, K. B., Huo, H., Kannari, A., Klimont, Z., Park, I. S., Reddy, S., Fu, J. S., Chen, D., Duan, L., Lei, Y., Wang, L. T., and Yao, Z. L.: Asian emissions in 2006 for the NASA INTEX-B mission, Atmos. Chem. Phys., 9, 5131–5153, doi:10.5194/acp-9-5131-2009, 2009.

Zhang, R., Jing, J., Tao, J., Hsu, S.-C., Wang, G., Cao, J., Lee, C. S. L., Zhu, L., Chen, Z., Zhao, Y., and Shen, Z.: Chemical characterization and source apportionment of $PM_{2.5}$ in

ACPD
15, 14141–14169, 2015

Beijing: seasonal perspective, Atmos. Chem. Phys., 13, 7053–7074, doi:10.5194/acp-13-7053-2013, 2013.
Zhao, S., Ming, J., Sun, J., and Xiao, C.: Observation of carbonaceous aerosols during 2006–2009 in Nyainqêntanglha Mountains and the implications for glaciers, Environ. Sci. Pollut. R., 20, 5827–5838, 2013.
Zhuang, B. L., Li, S., Wang, T. J., Deng, J. J., Xie, M., Yin, C. Q., and Zhu, J. L.: Direct radiative forcing and climate effects of anthropogenic aerosols with different mixing states over China, Atmos. Environ., 79, 349–361, 2013.

ACPD
15, 14141–14169, 2015

Table 1. Summary of BC concentrations, number fraction of coated BC particles, and light absorption coefficient during different sampling periods.

	BC (mean ± SD, ng m^{-3})			Number fraction of coated BC (%)			Absorption (M m^{-1})		
	Pollution episode	Clean days	All	Pollution episode	Clean days	All	Pollution episode	Clean days	All
Average	390 ± 207	86 ± 101	160 ± 190	64.6 ± 4.9	57.7 ± 6.6	59.3 ± 6.9	3.7 ± 2.9	1.3 ± 1.6	2.1 ± 2.4
25th	219	40	50	63.1	53.1	54.3	1.4	0.7	0.8
50th	410	68	80	65.6	58.3	60.2	3.4	0.9	1.2
75th	489	103	170	67.9	63.2	64.7	4.4	1.4	2.0

ACPD
15, 14141–14169, 2015

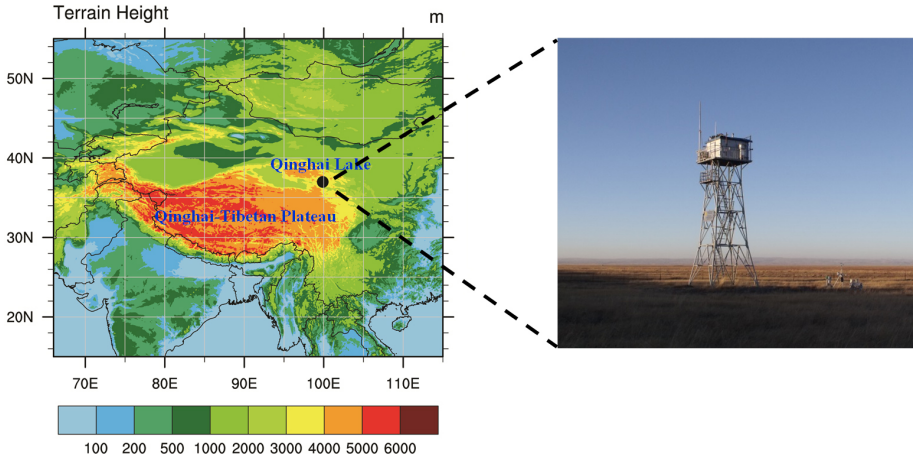

Figure 1. (left) Geographical location of Qinghai-Tibetan Plateau and surrounding areas. Color code represents topographical features (unit: m). (right) Observation tower at the "Bird Island" peninsula in Qinghai Lake, China.

ACPD
15, 14141–14169, 2015

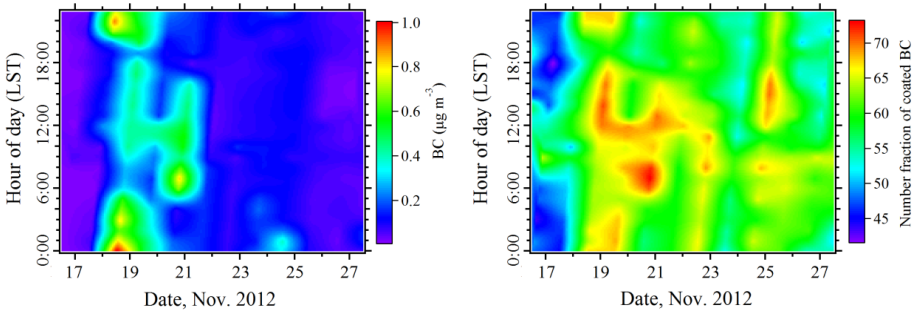

Figure 2. Hourly variations of BC mass concentration and number fraction of coated BC particles during the entire campaign.

ACPD
15, 14141–14169, 2015

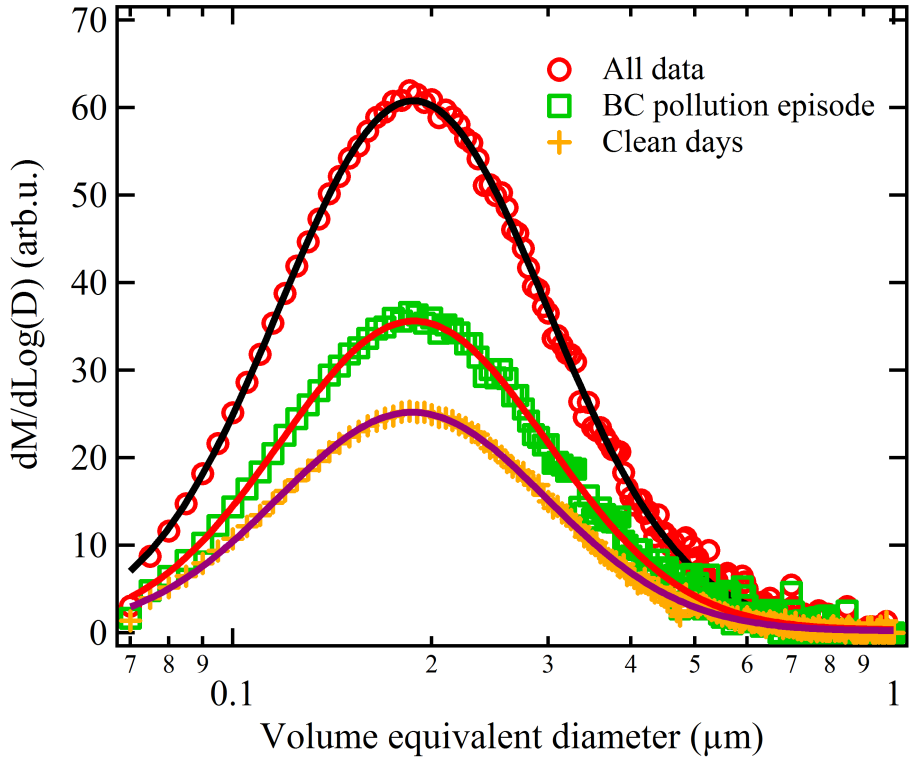

Figure 3. Mass size distribution of BC in volume equivalent diameter during different sampling periods at Qinghai Lake. The solid lines represent lognormal fit. "M" and "D" in vertical label represent BC mass and void free diameter (assuming 2 g cm^{-3} density), respectively.

ACPD
15, 14141–14169, 2015

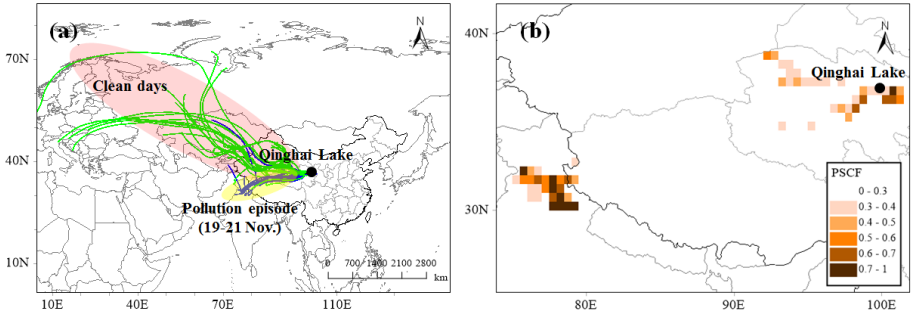

Figure 4. (a) Five-day backward air mass trajectories reaching at Qinghai Lake at 500 m above ground every six hours and **(b)** likely source areas of BC identified using potential source contribution function (PSCF) plots during the entire campaign.

ACPD
15, 14141–14169, 2015

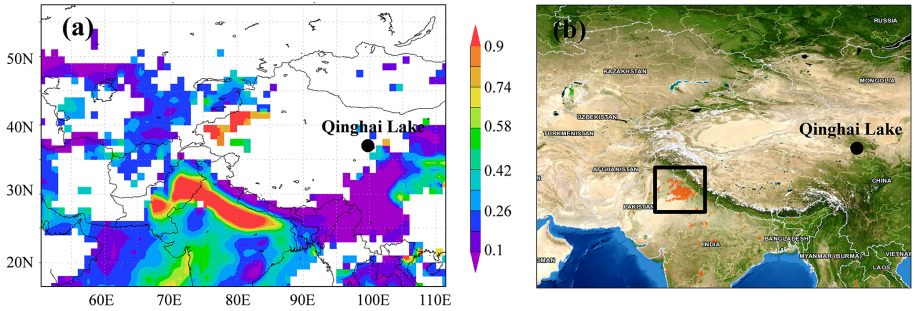

Figure 5. Regional distributions of **(a)** aerosol optical depth (AOD) and **(b)** fire counts map over Qinghai-Tibetan Plateau derived from MODIS observation during 14–16 November 2012.

ACPD
15, 14141–14169, 2015

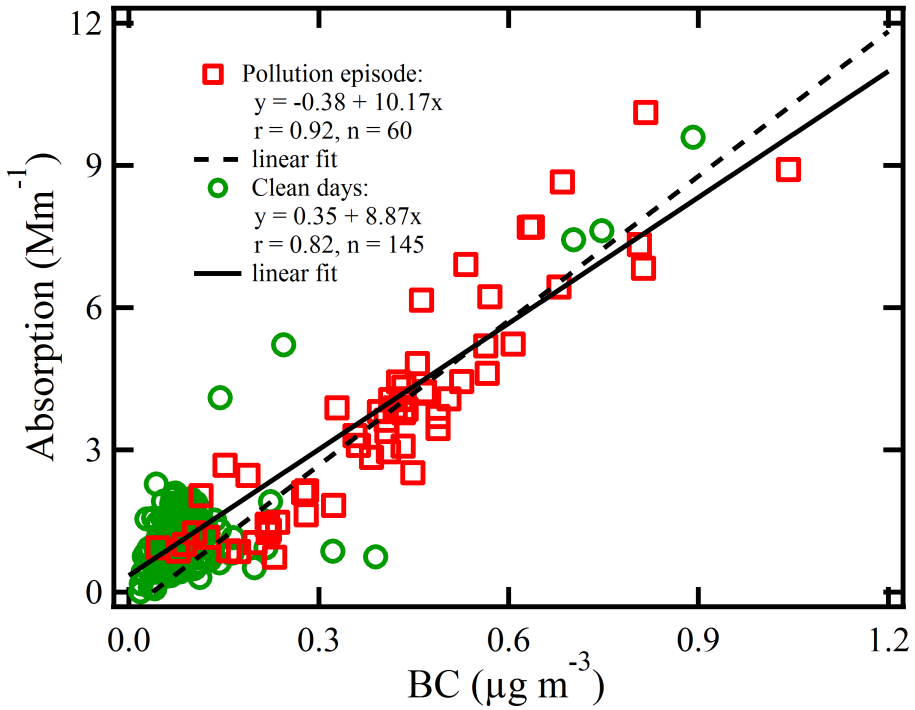

Figure 6. The linear relationship between light absorption and BC concentration during the pollution episode and clean days.

ACPD
15, 14141–14169, 2015

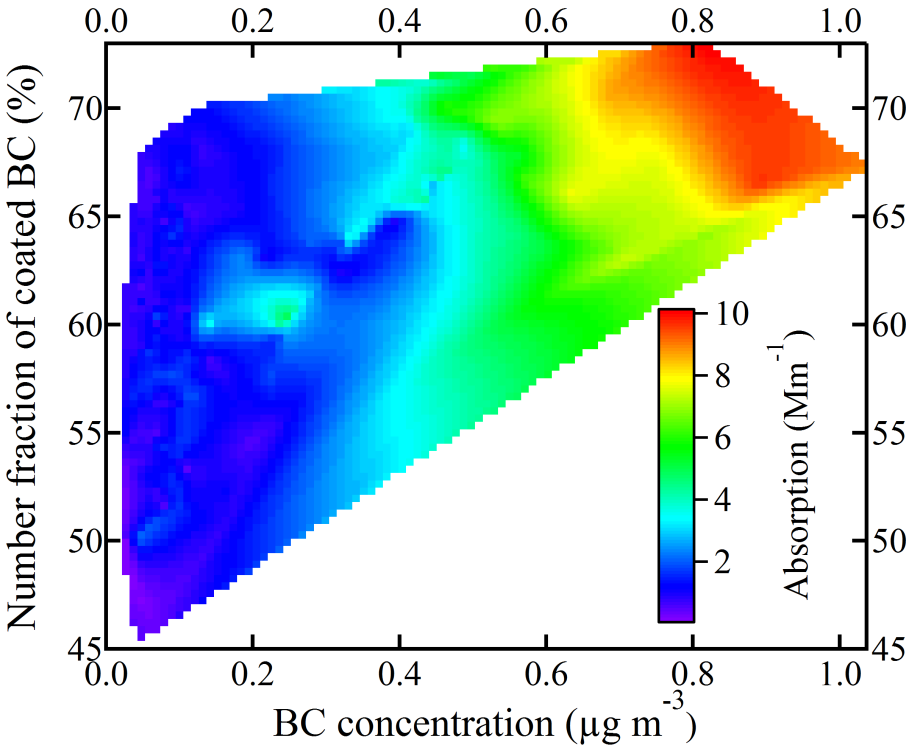

Figure 7. Relationship among BC concentration, number fraction of coated BC and light absorption coefficient during the campaign.

ACPD
15, 14141–14169, 2015